NULL PLACEMENT AND SIDELOBE SUPPRESSION IN FAILED ARRAY USING SYMMETRICAL ELEMENT FAILURE TECHNIQUE AND HYBRID HEURISTIC COMPUTATION

Shafqat U. Khan[1, *], Ijaz M. Qureshi[2, 4], Fawad Zaman[3], and Aqdas Naveed[3]

[1]School of Engineering & Applied Sciences, ISRA University, Islamabad, Pakistan

[2]Electrical Department, Air University, Islamabad, Pakistan

[3]Electronic Engineering Department, IIU, H-10, Islamabad, Pakistan

[4]Institute of Signals, Systems and Soft Computing (ISSS), Islamabad, Pakistan

Abstract—In this paper, we have addressed three major problems of uniform linear array in case of a sensor failure at any position. We assume that sensor position is known. The problems include increase in sidelobe levels, displacement of nulls and diminishing of null depth. The desired null depth is achieved by making the weight of symmetrical counterpart element passive. Genetic algorithm (GA) along with pattern search (PS) is used for reduction of sidelobe levels, and adjustment of nulls. Fitness function minimizing the error between the desired and estimated beam pattern along with null constraints is used. Simulation results for diversified scenarios have been given to demonstrate the validity and performance of the proposed algorithm.

1. INTRODUCTION

Null steering and beam steering are active research areas in the field of adaptive beamforming. Null steering is applied to suppress the unwanted signals in some specific direction. Thus it finds direct application in radar, sonar and mobile communication [1–3]. In literature various analytical and computational methods are available to address the issue of null steering [4–6]. The situation becomes

more challenging and complicated when an element fails in the active antenna array. The excitation of these elements is to achieve desired radiation pattern. In case of element failure, the sidelobe level (SLL) increase and nulls are displaced, which is highly undesirable. It is very expensive in terms of time and budget to replace the defective element frequently. Hence the weights of active elements in the same array should be recalculated and readjusted to create a new pattern close to the original one. Recently few algorithms have been proposed to correct the damaged pattern of the array [7–10]. In [7], Peter proposed a method to reconfigure the amplitude and phase distribution of the remaining elements by minimizing the average SLL through a conjugate gradient method, while in [8], Mailloux used the method of replacing the signals from failed elements in a digital beamforming receiving array. In [9, 10], the interference suppression and null steering techniques based on controlling the excitation amplitude only have been studied.

The importance of evolutionary computing (EC) and swarm intelligence in solving engineering problems has grown exponentially. Among EC techniques, genetic algorithm (GA) is considered to be one of the powerful and reliable tools to optimize the problems in any engineering field [11, 12]. GA is easy to understand and implement and avoids getting stuck in local minima. Yeo and Lu [13] proposed the genetic algorithms for array failure correction in digital beamforming of arbitrary arrays, while Rodriquez et al. [14] applied genetic algorithm to reduce the SLL for the failed array antenna. However, nulls steering and null depth are not taken into account, which are very important issues to be addressed. In [15], Basu and Mahanti used Firefly and artificial bees colony algorithm for synthesis of scanned and broadside linear array antenna. Grewal et al. [16] used the approach of Firefly algorithm for the reduction of SLL in failed array, while Ramsdale and Howerton [17], discussed the effects of element failure and random errors in amplitude and phase on the attainable sidelobe level with a linear array. Sim and Er [18] addressed the issue of sidelobe suppression for general arrays in the presence of element failures. GA [19] technique have been used for correcting element failures in antenna arrays. Latest work on null steering in failed antenna arrays is presented in [20]. The technique tries to restore the previous nulls pattern by using particle swarm optimization (PSO). All the above EC based techniques have discussed the SLL reduction and null steering in failed array, but no one is solving the issue of null depth and null steering at their original positions after failure of elements.

In this paper, the proposed algorithm addresses three major problems of uniform linear array in case of element failure. These

are increase in sidelobe levels, displacement of nulls and diminishing of null depth. We propose a symmetrical element failure (SEF) technique that provides better results in terms of null depth. Moreover, the SEF technique has deeper first null which is another big advantage over single element failure. The first null depth in beamforming is of great importance. To address the other two issues, we have used GA hybridized with pattern search (PS) to reduce the sidelobe levels and steer nulls back to their original positions by adjusting the current excitation of active sensors. GA is used as global optimizer whereas, pattern search is used as local optimizer. Various simulation results are provided to validate the performance of the proposed approach. The rest of the paper is organized as follows. The problem formulation is discussed in Section 2, while in Section 3 the proposed methodology structure is provided. Section 4 describes the simulations and results while Section 5 concludes the paper and proposes some future work.

2. PROBLEM FORMULATION

Consider a linear array in which all the elements are placed symmetrically about the origin. The total number of elements is $N = 2M + 1$. The array factor for this healthy set up with equally spaced elements, non-uniform amplitude and progressive phase excitation will be [21],

$$AF(\theta_i) = \sum_{n=-M}^{M} w_n \exp jn(kd\cos\theta_i + \alpha) \tag{1}$$

where w_n is the non-uniform weight of nth element whereas $n = 0, \pm 1, \pm 2, \ldots, \pm M$. The spacing between the adjacent elements is d, while θ is the angle from broadside. $k = 2\pi/\lambda$ is the wave number with λ as wavelength. The progressive phase shift α is given as

$$\alpha = -kd\cos\theta_s$$

where θ_s is steering angle for the main beam. The non-healthy array factor for single element failure is given by the expression below.

$$AF(\theta_i) = \sum_{n=-M}^{M} w_n \exp jn(kd\cos\theta_i + \alpha) \quad \text{for} \quad n \neq 9 \tag{2}$$

It is assumed that the w_9 element fails in the antenna array given in Fig. 1. One can clearly observe from Fig. 2, that due to single element failure the radiation pattern is damaged in terms of sidelobe levels, null depth and displacement of the nulls from their original position. So, the goal of this work is to recover the null depth, sidelobe levels, and null
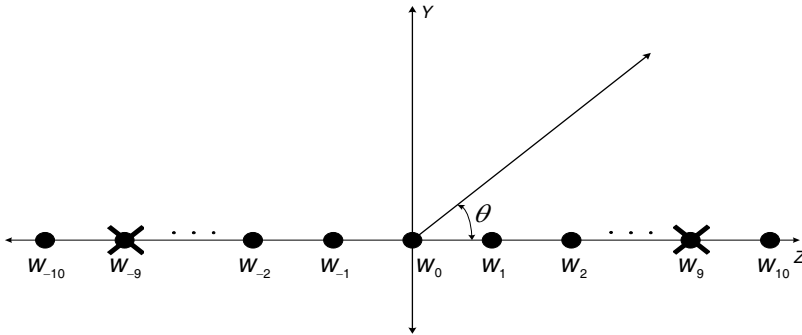
Figure 1. Non-uniform amplitude array of $2M + 1$ number of symmetry elements failure.
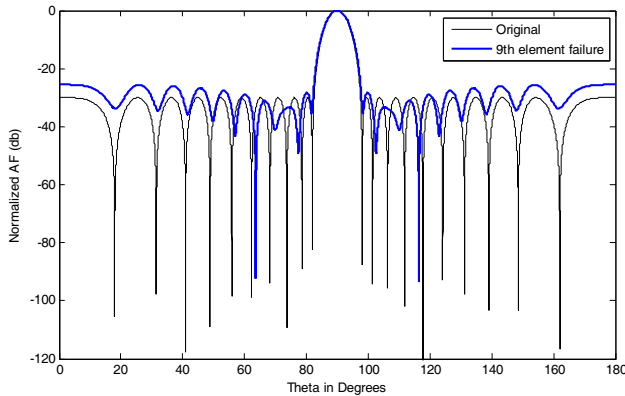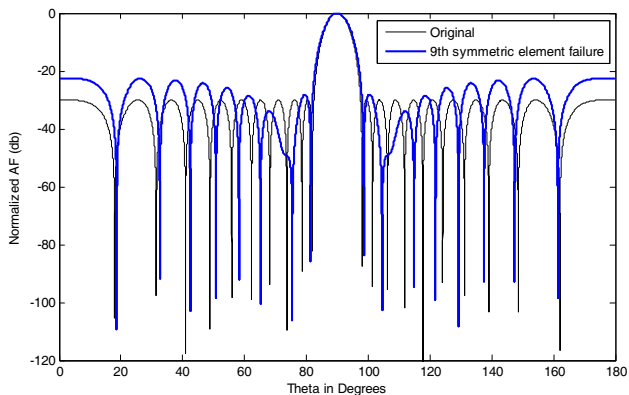

Figure 2. he initial 30-dB Chebyshev array and the w_9 element failure pattern.

placement at their original positions. Various methods are available in literature to correct the damage pattern of element failures, however, none of them is able to achieve the required null depth level.

3. PROPOSED METHODOLOGY

In this section, we develop the proposed methodology based on SEF. As we had assumed the failure of w_9 element, we lost the null depth as given in Fig. 2. For SEF technique we also force w_{-9} to be zero as depicted in Fig. 1. From Fig. 3, it is clear that symmetric element failure maintains the null depth almost as close to that of original array. The array factor for non-healthy symmetrical element failure is given

Figure 3. The initial 30-dB Chebyshev array and the (w_9, w_{-9}) symmetric element failure.

by,

$$AF(\theta_i) = \sum_{n=-M}^{M} w_n \exp jn(kd\cos\theta_i + \alpha) \quad \text{for} \quad n \neq \pm 9 \qquad (3)$$

Though, we have achieved better null depth level due to SEF, but the sidelobe levels and positioning of nulls is still an issue to be taken into account, for which we shall use the nature inspired evolutionary computing technique, i.e., GA for controlling sidelobe levels and placing the nulls towards required position.
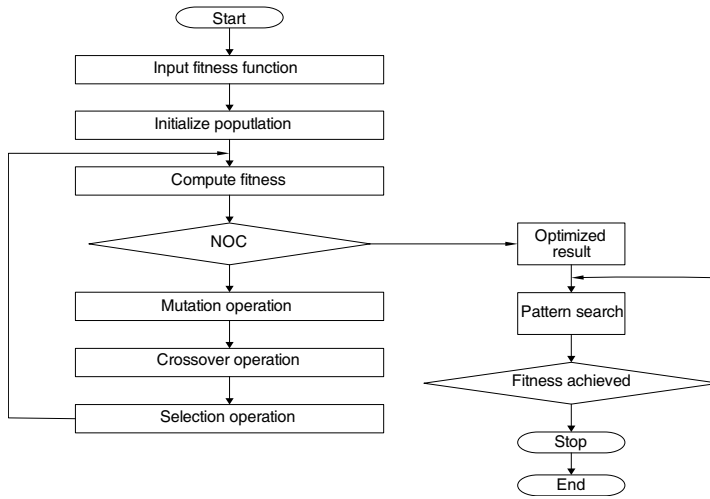
3.1. Genetic Algorithm (GA)

Evolutionary computation is basically a search for the fittest chromosome in the solution space. The flow chart for GA-PS is shown in Fig. 4, while the important steps are summarized below.

Step 1 Initialization: Generate K number of chromosomes randomly, each chromosome contain genes which represent current excitation of antenna elements.

Step 2 Fitness function: Calculate the fitness for each individual chromosome in the population. The fitness function depends on the mean square error (MSE) between the desired array factor and estimated array factor given in Equation (6) and the null constraint error given in Equation (7).

Step 3 Termination Criteria for GA: Program for GA terminates when maximum number of cycles (NOC) is reached and moves to step 5.

Figure 4. The flow diagram of genetic algorithm along with pattern search.

Table 1. Parameters used for PS and GA.

PS		GA	
Parameters	**Settings**	**Parameters**	**Setting**
Poll method	GPS Positive Np1	Population size	200
Polling order	Random	No of Generation	500
Mesh size	01	Migration Direction	Forward
Expansion Factor	2.0	Crossover fraction	0.2
Function Evaluation	13000	Crossover	Scattered
Maximum iteration	500	Function Tolerance	10^{-10}
Penalty Factor	100	Initial range	[0–1]
Contraction Factor	0.5	Scaling function	Rank
Mesh Tolerance	10^{-6}	Selection	Roulette
X Tolerance	10^{-6}	Elite count	2
Bind Tolerance	10^{-3}	Mutation function	Adaptive feasible

Step 4 Reproduction: Use the operators of elitism, crossover and mutation selection as shown in Table 1, to move from previous generation to the next improved generation. Go back to step 2.

Step 5 Refinement: PS algorithm is used for further tuning of results. The best individual of GA is given as a starting point to PS algorithm.

   Step 6 Termination of program: When fitness function achieves a certain prescribed value, the program terminates and stores the best chromosome, otherwise it goes back to step 5.

3.2. Pattern Search (PS)

PS algorithm does not need the gradient of the problem. The goal of PS is to compute a sequence of points that reach for an optimal point. In each step, the technique attempts to find out a set of points, called mesh, around the optimal point of the previous step. The mesh can be obtained by adding the current point to a scalar multiple of vectors called a pattern [22]. The new point becomes the current point in the next step of algorithm, if the PS finds the point in the mesh that improves the objective function at the current point. PS method is very successful for optimization problem such as, bound constrained minimization and globally convergent augmented lagrangian algorithm [23].

3.3. Null Constraint (NC)

In satellite, radar and mobile communication applications, a jamming signal located at a specific angle needs to be eliminated. For an arbitrary array, to put a null at a given angle θ_i, we need [24],

$$A(\theta_i) = \mathbf{w}^H \mathbf{v}(\theta_i) = 0 \qquad (4)$$

where

$$\mathbf{v}(\theta_i) = \begin{bmatrix} \exp\left(-j(\frac{N-1}{2})kd\cos\theta_i\right) \\ \exp\left(-j(\frac{N-3}{2})kd\cos\theta_i\right) \\ \vdots \\ \exp\left(j(\frac{N-3}{2})kd\cos\theta_i\right) \\ \exp\left(j(\frac{N-1}{2})kd\cos\theta_i\right) \end{bmatrix}_{N \times 1}$$

and $\mathbf{w}$ is $N \times 1$ vector which is defined as

$$\mathbf{w} = [w_{-M}, \ldots, w_0, \ldots, w_M]^T$$

The null constraint is given as

$$\mathbf{w}^H \mathbf{v}(\theta_i) = 0, \quad i = 1, 2, \ldots, M_0$$

We may define an $N \times M_0$ constraint matrix, $\mathbf{C}$ as

$$\mathbf{C} = [\mathbf{v}(\theta_1), \mathbf{v}(\theta_2), \ldots, \mathbf{v}(\theta_{M_0})] \qquad (5)$$

where θ_i for $i = 1, 2, \ldots, M_0$ is the direction of null. Our objective is to optimize the squared weighting error subject to the constraint that

$$\mathbf{w}^H \mathbf{C} = \mathbf{0}$$

Our requirement is that the columns of $\mathbf{C}$ should be orthogonal to the weight vector $\mathbf{w}$. Accordingly we may define G_i, $i = 1, 2$ and G as follows.

$$G_1 = \sum_{i=1}^{P} [\|AF_{GA}(\theta_i) - AF_d(\theta_i)\|]^2 \tag{6}$$

$$G_2 = \|\mathbf{w}^H \mathbf{C}\|^2 \tag{7}$$

$$G = G_1 + G_2 \tag{8}$$

Hence G is the fitness function for the problem given above which are to be minimized Best chromosome shall give the minimal value of G. The first term in (8) is used for SLL reduction, where $AF_d(\theta_i)$ represent the desired pattern and $AF_{GA}(\theta_i)$ is the pattern obtained by using GA. The second term in (8) is used for jammer suppression and placement of nulls at their original positions after element failure.

4. SIMULATION RESULTS

In simulation, a Classical Dolph-Chebyshev linear array of 21 elements with $\lambda/2$ inter-element spacing is used as the test antenna. The array factor in this case represents a $-30\,\text{dB}$ constant SLL with the nulls at specific angles. Analytical techniques are used to find out the non-uniform excitations for Classical Dolph-Chebyshev array. In case of element failure, GA is used to suppress the SLL and place the nulls to their original positions by recalculating and adjusting the weights of remaining active elements.

Case 1: At the first instant the element failure in the antenna array is assumed to be w_9. After element failure the radiation pattern is destroyed, which results in increase of the SLL and displacement of null positions. In order to regain the symmetry, its mirror element weight w_{-9} is forced to zero. We achieve the required null depth level (NDL) and deeper first null depth level (FNDL) as compared to that of non-symmetric case. The SLL rises to $-25.64\,\text{dB}$ due to the w_9 element failure, while due to SEF of the w_9 element, the SLL is $-24.18\,\text{dB}$. The advantage of SEF is deeper nulls, especially, the first null. The SLL and FNDL for damage array of single element failure and SEF are shown in Table 2. It is clear from Fig. 3 that SEF maintains better FNDL as compared to that of single element failure.

After optimization by GA, the SLL of the w_9 element failure are reduced to $-28.1\,\text{dB}$ while due to SEF, the SLL is reduced to $-27.93\,\text{dB}$. The recovery of one null due to single element failure and SEF to its original position $\theta_1 = 18°$ are shown in Figs. 5 and 6. The comparison of recovered pattern with single element and SEF for one

Table 2. Comparison of FNDL and SLL for the damaged pattern.

Comparison of FNDL and SLL of damage pattern of one element and SEF			
One element failure		SEF	
FNDL (dB)	SLL (dB)	FNDL (dB)	SLL (dB)
−34.8	−25.64	−85.63	−24.17

Table 3. Recovery of one null.

| Comparison of NDL and SLL of one element failure and SEF				
Correction of one element failure		Correction of SEF		Recovery of Nulls
NDL (dB)	SLL (dB)	NDL (dB)	SLL (dB)	
−115.3	−27.66	−116.4	−27.93	1st null recovered.
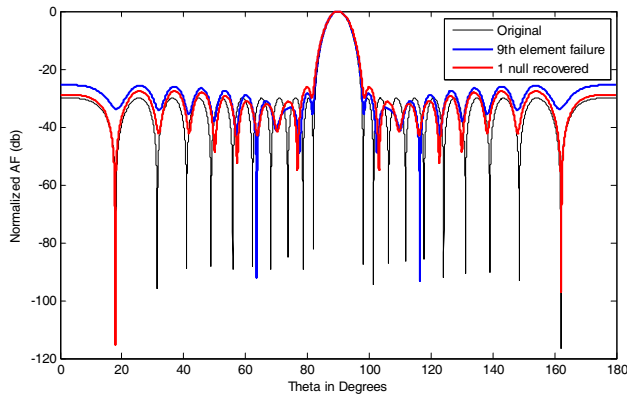
Figure 5. Radiation pattern for original, the w_9 element failure and one null recovery.

null imposed is given in Table 3. The recovered NDL of SEF is one dB deeper than that of single element failure.

Figures 7 and 8 show the recovery of three nulls orginally at angles of $\theta_1 = 18°$, $\theta_2 = 31.43°$ and $\theta_3 = 40.94°$ for single element failure and SEF. The SLL and NDL for the corresponding nulls are given in Table 4. The NDL in SEF is one dB deeper than that of single element failure.
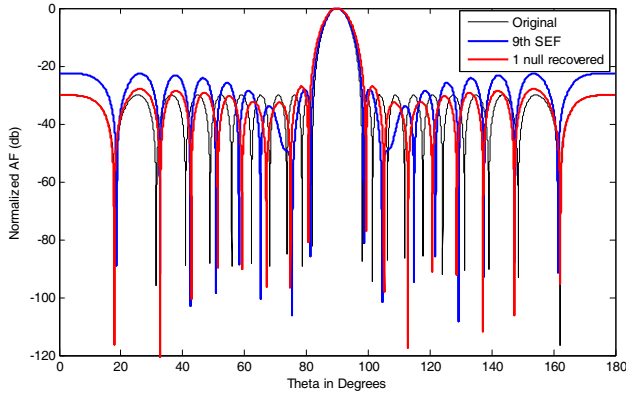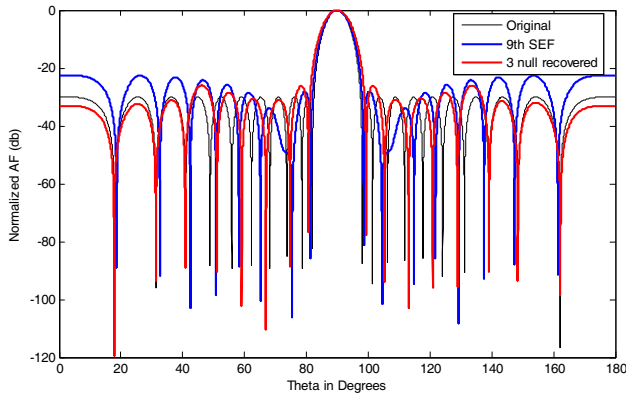
Figure 6. Radiation pattern for original and the (w_9, w_{-9}) SEF and one null recovery.
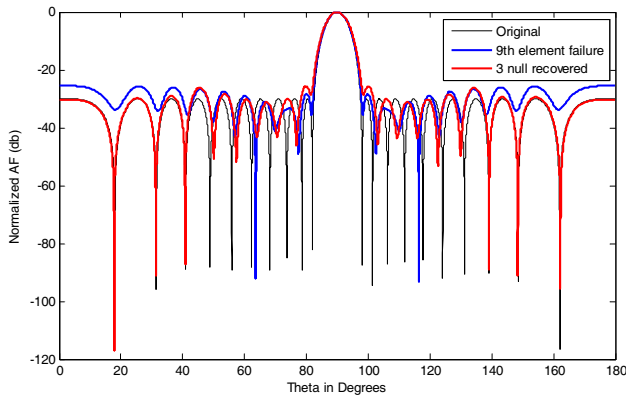
Figure 7. Radiation pattern for original, the w_9 element failure and three nulls recovery.

Now the recovery of six nulls for single element failure and SEF originally at positions $18°$, $31.43°$, $40.94°$, $48.83°$, $55.85°$ and $68.19°$ is carried out and shown in Figs. 9 and 10. A comparison of SLL and NDL for the recovery of six nulls is given in Table 5. In each case SEF produces deeper nulls compared to the single element failure. From simulation it is observed that we have received deeper first null in SEF scenarios discussed above.

Case 2: In this case, the w_7 element is assumed to fail. Due to symmetry its mirror element weight w_{-7} is forced to zero. For single element failure the SLL is increased to -23.95 dB, while due to the w_7 SEF, SLL is increased to -20.55 dB, which is the price to be paid
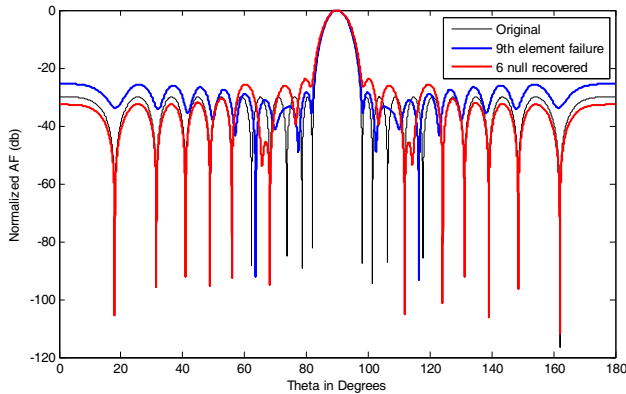
Figure 8. Radiation pattern for original, the (w_9, w_{-9}) SEF and three nulls recovery.

Table 4. Recovery of three nulls.

Comparison of NDL and SLL of one element failure and SEF				
Correction of one element failure		Correction of SEF		Recovery of Nulls
NDL (dB)	SLL (dB)	NDL (dB)	SLL (dB)	
−116.4	−29.5	−120.2	−32.03	One null recovered.
−92.44	−29.42	−94.3	−31.38	2nd null recovered.
−88.19	−26.91	−89.58	−26.4	3rd null recovered.

Table 5. Recovery of six nulls.

| Comparison of NDL and SLL of one element failure and SEF				
Correction of one element failure		Correction of SEF		Recovery of Nulls
NDL (dB)	SLL (dB)	NDL (dB)	SLL (dB)	
−105.4	−32.52	−116.1	−43.38	One null recovered.
−95.01	−32.75	−105.8	−43.08	2nd null recovered.
−92.04	−32.08	−101.4	−42.4	3rd null recovered.
−95.31	−30.73	−100.2	−40.33	4th null recovered.
−92.44	−25.94	−96.48	−36.72	5th null recovered.
−94.7	−26.65	−96.8	−29.75	6th null recovered

Figure 9. Radiation pattern for original, the w_9 element failure and six nulls recovery.
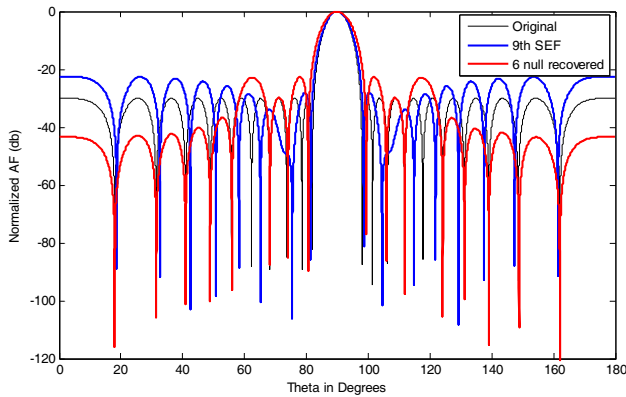

Figure 10. Radiation pattern for original, the (w_9, w_{-9}) SEF and six nulls recovery.

to achieve deeper nulls including the first null. After optimization the amplitudes and phases of the remaining active elements were adjusted by using GA with PS to achieve the radiation pattern close to the desired one. The SLL is reduced to as -26.36 dB, while due to SEF, the SLL is reduced to 23.9 dB. In case of the w_9 symmetry element failure the number of achievable nulls are eight, while due to the w_7 symmetry element failure only six nulls are achieved. The SLL and beamwidth of the w_7 SEF is slightly greater than that of the w_9 SEF. The number of nulls received in the w_7 SEF is two less than that of the w_9 SEF. The number of nulls reduces in SEF as failure element moves towards the centre element. The original and the w_7 element
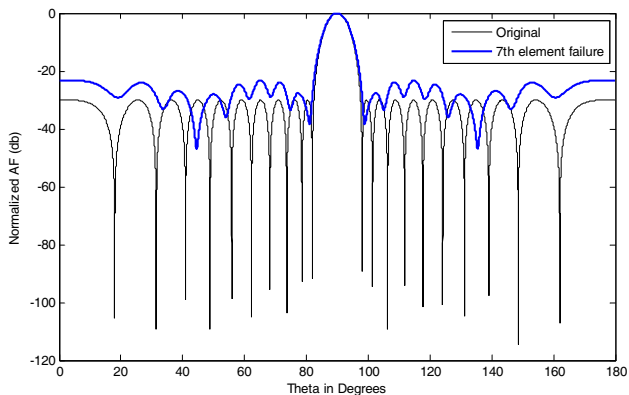
Figure 11. The original Chebyshev array, the w_7 element failure pattern.
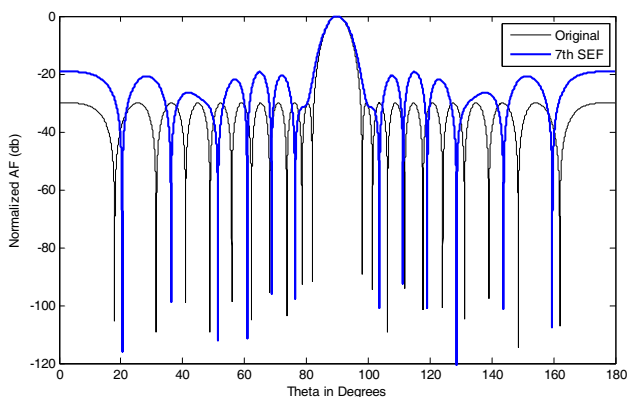

Figure 12. The original Chebyshev and the (w_7, w_{-7}) symmetry element failure pattern.

failure pattern are shown in Fig. 11, while the original and SEF pattern are shown in Fig. 12. The comparison of FNDL and SLL for the w_7 element failure and SEF is given in Table 6. The FNDL of the w_7 SEF is deeper than that of single element failure along with other deeper nulls in SEF. From the simulation result it is concluded that if the element failure occurs near the centre element, the number of nulls reduces by one on both sides of main beam.

   After optimization the SLL of w_7 element failure are reduced to $-29.07\,\mathrm{dB}$ while due to SEF, the SLL is $-27.13\,\mathrm{dB}$ and the recovery of one null is imposed at $\theta_1 = 18°$. Figs. 13 and 14 show the recovery

Table 6. Comparison of FNDL and SLL for damaged pattern.

Comparison of FNDL and SLL of damage pattern of one element and SEF			
One element failure		SEF	
FNDL (dB)	SLL (dB)	FNDL (dB)	SLL (dB)
-37.23	-27.59	-84.48	-24.88
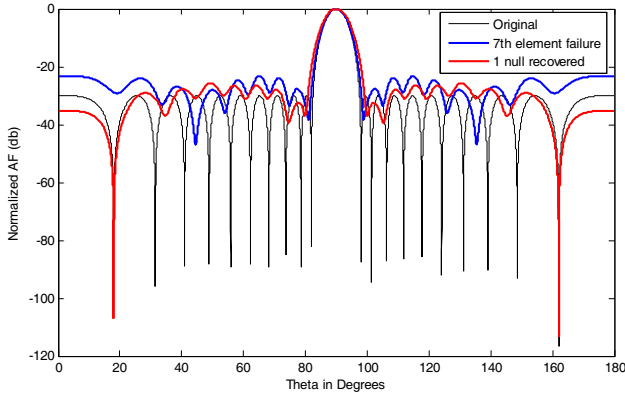
Figure 13. Radiation pattern for original, the w_7 element failure and one null recovery.
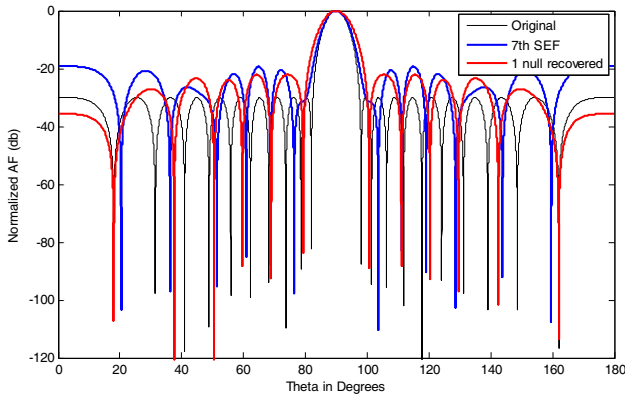
Figure 14. Radiation pattern for original, the (w_7, w_{-7}) SEF and one null recovery.
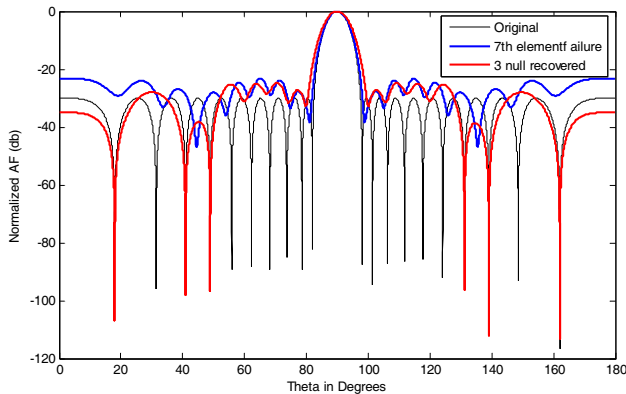
of one null for single element failure and SEF. The comparison of NDL and SLL is given in Table 7. The NDL of SEF is one dB deeper than single element failure. The SEF gives better FNDL and deeper nulls

Table 7. Recovery of one null.

Comparison of NDL and SLL of one element failure and SEF				
Correction of one element failure		Correction of SEF		Recovery of Nulls
NDL (dB)	SLL (dB)	NDL (dB)	SLL (dB)	
−106.2	−29.07	−107.3	−27.13	One null recovered.

Table 8. Recovery of three nulls.

| Comparison of NDL and SLL of one element failure and SEF				
Correction of one element failure		Correction of SEF		Recovery of Nulls
NDL (dB)	SLL (dB)	NDL (dB)	SLL (dB)	
−106.8	−29.94	−108.1	−25.7	1st null recovered.
−97.94	−39.37	−101.2	−33.28	2nd null recovered.
−96.7	−25.6	−102.3	−24.91	3rd null recovered.

Figure 15. Radiation pattern for original, the w_7 element failure and three nulls recovery.

than single element failure.

Figures 15 and 16 show the recovery of three nulls at angles of $\theta_1 = 18°$, $\theta_2 = 40.94°$ and $\theta_3 = 48.83°$ respectively for single element failure and SEF. The SLL and NDL for the corresponding nulls is
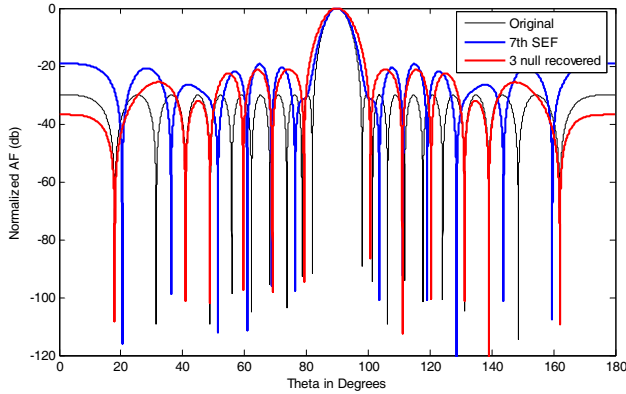
Figure 16. Radiation pattern for original, the (w_7, w_{-7}) SEF and three nulls recovery.
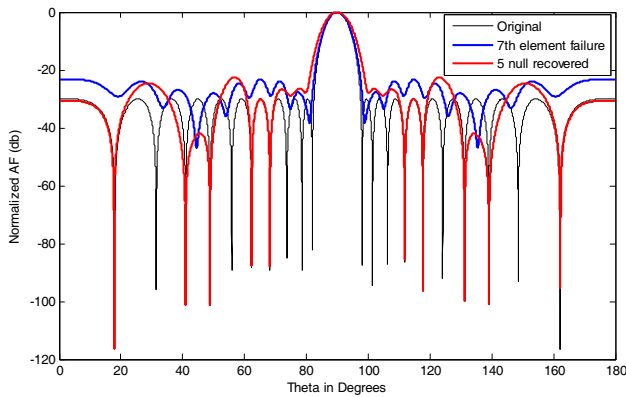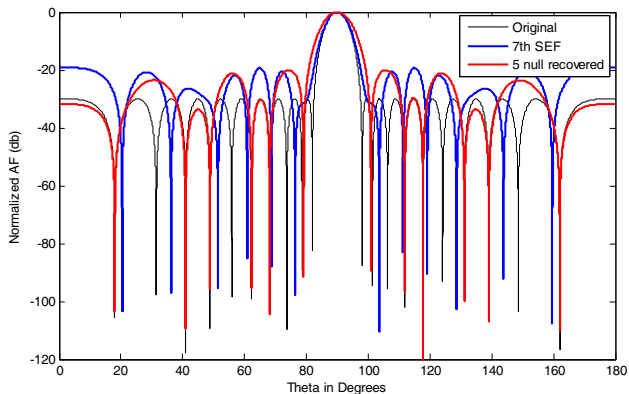

**Figure 17.** Radiation pattern for original, the w_7 element failure and five nulls recovery.

given in Table 8. The NDL of the 3rd null in SEF is six dB deeper as compared to the single element failure.

Figures 17 and 18 show the original, damage and corrected pattern of five nulls recovered for single element failure and SEF. The recovery of five nulls which are placed at $18°$, $40.94°$, $48.83°$, $62.25°$ and $68.19°$ positions. The comparison of SLL and NDL for the recovery of five nulls is given in Table 9. The NDL of the 5th null in SEF is deeper than single element failure.

Case 3: The main beam can be directed at any angle. If the user changes their position then the main beam can be steered in the

Figure 18. Radiation pattern for original, the (w_7, w_{-7}) SEF and five nulls recovery.
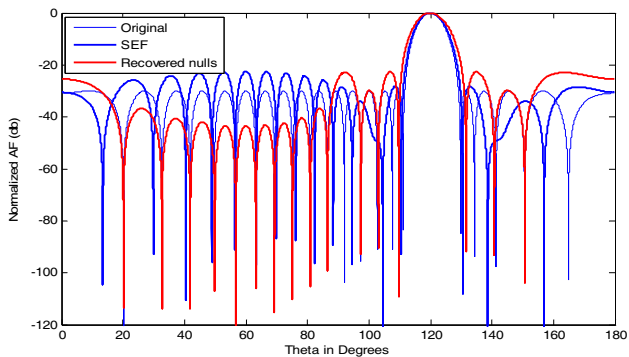
Figure 19. Corrected pattern with main beam pointing at $120°$ with recovered nulls.

desired direction. Fig. 19 shows the corrected pattern with recovered nulls at main beam pointing that is, at $\theta_s = 120°$. The main beam can be steered in the direction of desired user at any angle. The array factor for $2M + 1$ elements in terms of main beam direction θ_s is given by

$$AF(\theta_i) = \sum_{n=-M}^{M} w_n \exp jnkd \left(\cos\theta_i - \cos\theta_s\right)$$

where θ_s is the main beam direction to which it can be steered to different angles.

Table 9. Recovery of five nulls.

Comparison of NDL and SLL of one element failure and SEF				
Correction of one element failure		Correction of SEF		Recovery of Nulls
NDL (dB)	SLL (dB)	NDL (dB)	SLL (dB)	
−116.5	−24.64	−101.8	−23.87	1st null recovered.
−101.3	−42.18	−109.4	−33.61	2nd null recovered.
−101.3	−23.16	−95.48	−21.59	3rd null recovered.
−87.54	−30.5	−95.21	−31.56	4th null recovered.
−87.4	−27.85	−104.5	−20.5	5th null recovered.

5. CONCLUSION AND FUTURE WORK

We have proposed symmetric element failure (SEF) technique along with hybrid evolutionary computational method for the correction of failed element array. The null depth of all nulls, especially the first one, has been achieved with the help of SEF technique. Null placement and sidelobe suppression have been achieved by hybridizing GA with PS and using a proper fitness function demanding the sidelobe suppression and null constraints. The simulation result shows that as the faulty element gets near the centre element, the number of nulls reduces. The reduction in the corrected side lobe level comes at the cost of broader main beam. The corrected pattern has beamwidth broader than that of the original. Using the approach of mirror/symmetric element failure, with the reduction of SLL, we can steer single, double and multiple nulls in the direction of known interferences. This method can be extended to planar arrays.

REFERENCES

1. Applebaum, S. P., "Adaptive arrays," *IEEE Transactions on Antennas and Propagation*, Vol. 24, No. 9, 585–598, Sep. 1976.
2. Hejres, J. A., "Null steering in phased arrays by controlling the position of selected elements," *IEEE Transactions on Antennas and Propagation*, Vol. 52, No. 11, Nov. 2004.
3. Krim, H. and M. Viberg, "Two decades of array signal processing research," *IEEE Signal Processing M*, 67–94, Jul. 1996.
4. Khan, Z. U., A. Naveed, I. M. Qureshi, and F. Zaman,

"Independent null steering by decoupling complex weights," *IEICE Electronic Express*, Vol. 8, No. 13, 1008–1013, 2011.

5. Hejres, J. A., A. Peng, and J. Hijres, "Fast method for sidelobe nulling in a partially adaptive linear array using the elements positions," *IEEE Antennas and Wireless Propagation Letters*, Vol. 6, 332–335, 2007.

6. Hejres, J. A., "Null steering in phased arrays by controlling the position of selected elements," *IEEE Transactions on Antennas and Propagation*, Vol. 52, No. 11, Nov. 2004.

7. Peters, T. J., "A conjugate gradient-based algorithm to minimize the sidelobe level of planar arrays with element failures," *IEEE Transactions on Antennas and Propagation*, Vol. 39, 1497–1504, Oct. 1991.

8. Mailloux, R. J., "Array failure correction with a digitally beamformed array," *IEEE Transactions on Antennas and Propagation*, Vol. 44, 1542–1550, Dec. 1996.

9. Guney, K. and S. Basbug, "Interference suppression of linear antenna arrays by amplitude-only control using a bacterial foraging algorithm," *Progress In Electromagnetics Research*, Vol. 79, 475–497, 2008.

10. Guney, K. and M. Onay, "Amplitude-only pattern nulling of linear antenna arrays with the use of bees algorithm," *Progress In Electromagnetics Research*, Vol. 70, 21–36, 2007.

11. Zaman, F., I. M. Qureshi, A. Naveed, J. A. Khan, and M. A. Z. Raja, "Amplitude and directional of arrival estimation: Comparison between different techniques," *Progress In Electromagnetics Research B*, Vol. 39, 319–335, 2012.

12. Zaman, F., I. M. Qureshi, A. Naveed, and Z. U. Khan, "Joint estimation of amplitude, direction of arrival and range of near field sources using memetic computing," *Progress In Electromagnetics Research C*, Vol. 31, 199–213, 2012.

13. Yeo, B. K. and Y. Lu, "Array failure correction with a genetic algorithm," *IEEE Transactions on Antennas and Propagation*, Vol. 47, No. 5, 823–828, 1999.

14. Rodriquez, J. A., F. Ares, and E. Moreno, "Genetic algorithm procedure for linear array failure correction," *Electronic Letters*, Vol. 36, No. 3, 196–198, 2000.

15. Basu, B. and G. K. Mahanti, "Fire fly and artificial bees colony algorithm for synthesis of scanned and broadside linear array antenna," *Progress In Electromagnetics Research B*, Vol. 32, 169–190, 2011.

16. Grewal, N. S., M. Rattan, and M. S. Patterh, "A linear antenna array failure correction using firefly algorithm," *Progress In Electromagnetics Research M*, Vol. 27, 241–254, 2012.

17. Ramsdale, D. J. and R. A. Howerton, "Effect of element failure and random errors in amplitude and phase on the sidelobe level attainable with a linear array," *J. Acoust, Soc. Am.*, Vol. 68, No. 1, 901–906, 1980.

18. Sim, S. L. and M. H. Er, "Sidelobe suppression for general arrays in presence of element failures," *Electronics Letters*, Vol. 33, No. 15, 1278–1280, 1997.

19. Yeo, B.-K. and Y. Lu, "Array failure correction with a genetic algorithm," *IEEE Transactions on Antennas and Propagation*, Vol. 47, No. 5, 823–828, May 1999.

20. Acharya, O. P., A. Patnaik, and S. N. Sinha, "Null steering in failed antenna arrays," *Applied Computational Intelligence and Soft Computing*, Vol. 2011, Article ID. 692197, 9 pages, 2011.

21. Wolf, I., "Determination of the radiating system which will produce a specified directional characteristic," *Proc. IRE*, Vol. 25, 630–643, May 1937.

22. Torczon, V., "On the convergence of pattern search algorithms," *SIAM Journal on Optimization*, Vol. 7, No. 1, 1–25, 1997.

23. Taddy, M. A., H. K. H. Lee, G. A. Gray, and J. D. Griffin, "Bayesian guided pattern search for robust local optimization," *Technometrics*, Vol. 51, No. 4, 389–401, 2009.

24. Steyskal, H., R. Shore, and R. Haupt, "Methods for null control and their effects on the radiation pattern," *IEEE Transactions on Antennas and Propagation*, Vol. 34, No. 3, 404–409, 1986.